PHYSICAL REVIEW C **90**, 011306(R) (2014)

Impact of variational space on $M1$ transitions between first and second quadrupole excitations in ^{132,134,136}Te

A. P. Severyukhin,[1,*] N. N. Arsenyev,[1] N. Pietralla,[2] and V. Werner[2]

[1]*Bogoliubov Laboratory of Theoretical Physics, Joint Institute for Nuclear Research, 141980 Dubna, Moscow Region, Russia*

[2]*Institut für Kernphysik, Technische Universität Darmstadt, 64289 Darmstadt, Germany*

(Received 3 April 2014; revised manuscript received 4 July 2014; published 28 July 2014)

$M1$ transitions between low-energy quadrupole excitations of the valence shell are often used as the signature for states of proton-neutron mixed-symmetry character. Starting from the Skyrme interaction f_- together with the volume pairing interaction, we study the properties of the $2^+_{1,2}$ excitations of ^{132,134,136}Te. The coupling between one- and two-phonon terms in the wave functions of excited states is taken into account. Our calculations are performed within the finite-rank separable approximation, which enables one to perform quasiparticle random phase approximation calculations in very large two-quasiparticle configurational spaces. Using the same set of parameters we describe available experimental data and give the prediction for ^{136}Te, $B(M1;\, 2^+_2 \rightarrow 2^+_1) = 0.51\mu_N^2$ in comparison to $0.30\mu_N^2$ in the case of ^{132}Te.

DOI: 10.1103/PhysRevC.90.011306 PACS number(s): 21.60.Jz, 21.10.Ky, 21.10.Re, 27.60.+j

Low-lying isovector excitations of the valence shell of heavy nuclei represent a unique laboratory for studying the balance among collectivity, shell structure, and isospin degree of freedom. These excitations, so-called mixed-symmetry (MS) states, have been predicted in the proton-neutron (pn) version of the interacting boson model (IBM-2) [1], where the pn symmetry of the wave functions is quantified by the bosonic analog of the isospin, termed F spin [2–5]. In particular, there are fully symmetric (FS) states with maximum F spin ($F = F_{\max}$) and MS states with $F < F_{\max}$. A rather complete list of references on that subject is given in a review [6]. Heyde and Sau described the FS and MS states in the framework of the schematic two-state model (TSM) [7], which has occasionally been used to estimate the properties of quadrupole states (see, e.g., Refs. [8,9]). The TSM consists of a neutron pair and a proton pair, each in a single-j subshell, thus, they are related to d-boson configurations in the IBM-2. Configurations with unperturbed energies are mixed by the residual neutron-proton interaction. The relative phases of proton and neutron amplitudes are opposite in the resulting first and second 2^+ states, i.e.,

$$|2^+_{\rm FS}\rangle = \alpha|2^+_\nu\rangle + \beta|2^+_\pi\rangle, \tag{1}$$

$$|2^+_{\rm MS}\rangle = -\beta|2^+_\nu\rangle + \alpha|2^+_\pi\rangle. \tag{2}$$

The amplitudes α and β may reflect two distinct situations: either $\alpha \approx \beta$, leading to well-developed FS and MS states, or $\alpha \neq \beta$. This unbalanced pn content of the wave functions can be interpreted as configurational isospin polarization (CIP) [9], which denotes varying contributions to the 2^+ states by active proton and neutron configurations due to the subshell structure. The CIP effect was first observed in ^{92,94}Zr [8,10–13].

Experiments on the $N = 80$ isotones ^{138}Ce [14], ^{136}Ba [15], ^{134}Xe [16], and ^{132}Te [17] revealed a systematic decrease in the excitation energy of the $2^+_{1,\rm MS}$ states with decreasing proton number, and the MS state is found as the 2^+_4, 2^+_3, and 2^+_2 state, respectively. For ^{138}Ce the $M1$ strength associated with the MS mode splits over two close-lying states, but no splitting is observed in ^{136}Ba. Large $B(M1;\, 2^+_{\rm MS} \rightarrow 2^+_1)$ values have been measured, with $0.26 \pm 0.03\mu_N^2$ in ^{136}Ba, $0.30 \pm 0.02\mu_N^2$ in ^{134}Xe, and the lower limit equal to $0.23\mu_N^2$ in ^{132}Te.

The low-energy quadrupole excitations of ^{132,134,136}Te show interesting properties. The good experimental knowledge of the remarkable reduction in the excitation energy and $B(E2)$ value of the first 2^+ state [18] of ^{136}Te with respect to ^{132}Te makes the properties of the 2^+_1 states of ^{132,134,136}Te an attractive topic for theoretical studies, based on either the mean-field method [19,20] or the shell model [21–25]. This anomaly has been attributed to the neutron dominance of the 2^+_1 state of ^{136}Te [19–25]. This means, based on Eqs. (1) and (2), that the 2^+ state of ^{136}Te with a predominantly MS character should be dominated by proton contributions within the TSM. Various shell-model calculations give conflicting results with respect to the $B(M1;\, 2^+_2 \rightarrow 2^+_1)$ value in ^{136}Te: Ref. [21] yields $B(M1;\, 2^+_2 \rightarrow 2^+_1) = 0.24\mu_N^2$, while Ref. [25] predicts a splitting of the MS 2^+ configuration between the 2^+_3 and the 2^+_4 state. It is worth mentioning that the first IBM-2 prediction of the $2^+_{1,2}$ energies of ^{132}Te was done in Ref. [26].

It would be helpful to study the effect of the variational configuration space on the behavior of the $B(M1;\, 2^+_2 \rightarrow 2^+_1)$ value of Te isotopes. Our tool is the quasiparticle random phase approximation (QRPA) with Skyrme interactions in a separable approximation [20]. Making use of the finite-rank separable approximation [27] for the residual interaction enables us to perform QRPA calculations in very large two-quasiparticle (2QP) spaces. In particular, the cutoff of the discretized continuous part of the single-particle (SP) spectra is at the energy of 100 MeV. Because of this large configurational space, we do not need effective charges. Taking into account the basic ideas of the quasiparticle-phonon model (QPM) [28,29], the Hamiltonian is then diagonalized in a space spanned by states composed of one and two QRPA phonons

*sever@theor.jinr.ru

[30,31],

$$\Psi_\nu(\lambda\mu) = \left(\sum_i R_i(\lambda\nu) Q^+_{\lambda\mu i} + \sum_{\lambda_1 i_1 \lambda_2 i_2} P^{\lambda_1 i_1}_{\lambda_2 i_2}(\lambda\nu) \left[Q^+_{\lambda_1 \mu_1 i_1} Q^+_{\lambda_2 \mu_2 i_2} \right]_{\lambda\mu} \right) |0\rangle, \quad (3)$$

where λ denotes the total angular momentum and μ is its z projection in the laboratory system. The ground state is the QRPA phonon vacuum $|0\rangle$ and the wave functions of the one-phonon excited states given by $Q^+_{\lambda\mu i}|0\rangle$ as a superposition of 2QP configurations. The normalization condition of the one-phonon excited states leads to the relation

$$\frac{1}{2} \sum_{jj'} \left(X^{\lambda i}_{jj'} X^{\lambda i'}_{jj'} - Y^{\lambda i}_{jj'} Y^{\lambda i'}_{jj'} \right) = \delta_{ii'} \quad (4)$$

of the phonon amplitudes (X,Y) [20,32]. The index j is a short notation for the familiar quantum numbers nlj. The wave functions of excited states, (3), are composed of a mixture of 2QP and four-quasiparticle configurations that form the one-phonon and two-phonon components. In order to let the two-phonon components of the wave functions, (3), obey the Pauli principle we take into account exact commutation relations between the phonon operators, as proposed in Ref. [28]. In particular, the normalization condition of the wave functions, (3), can be written as

$$\sum_i R_i^2(\lambda\nu) + 2 \sum_{\lambda_1 i_1 \lambda_2 i_2} \left(P^{\lambda_1 i_1}_{\lambda_2 i_2}(\lambda\nu) \right)^2 (1 + K^\lambda(\lambda_1 i_1, \lambda_2 i_2)) = 1,$$

$$K^\lambda(\lambda_1 i_1, \lambda_2 i_2) = (2\lambda_1 + 1)(2\lambda_2 + 1) \times \frac{1}{1 + \delta_{\lambda_1 i_1, \lambda_2 i_2}} \sum_{j_1 j_2 j_3 j_4} (-1)^{j_2 + j_4 + \lambda} \begin{Bmatrix} j_1 & j_2 & \lambda_2 \\ j_4 & j_3 & \lambda_1 \\ \lambda_1 & \lambda_2 & \lambda \end{Bmatrix} \times \left(X^{\lambda_1 i_1}_{j_1 j_4} X^{\lambda_1 i_1}_{j_3 j_4} X^{\lambda_2 i_2}_{j_3 j_2} X^{\lambda_2 i_2}_{j_1 j_2} - Y^{\lambda_1 i_1}_{j_1 j_4} Y^{\lambda_1 i_1}_{j_3 j_4} Y^{\lambda_2 i_2}_{j_3 j_2} Y^{\lambda_2 i_2}_{j_1 j_2} \right). \quad (5)$$

The amplitudes $R_i(\lambda\nu)$ and $P^{\lambda_1 i_1}_{\lambda_2 i_2}(\lambda\nu)$ are determined from the variational principle, which leads to a set of linear equations. The equations have the same form as the QPM equations [28,33], but the SP spectrum and the parameters of the residual interaction are calculated with the chosen Skyrme forces without any further adjustments. The density of SP states near the Fermi level is related to the neutron and proton effective masses of the mean-field Hamiltonian. As the parameter set in the particle-hole channel, we use the Skyrme force f_- [34]. It predicts in a symmetric matter an effective mass of 0.7, with negative isospin splitting of the effective mass in neutron-rich systems, $m_n^* < m_p^*$. The pairing correlations are generated by a zero-range volume force with a strength of -280 MeV fm^3 and a smooth cutoff at 10 MeV above the Fermi energies [20,31]. This value of the pairing strength has been fitted to reproduce the experimental pairing energies of ^{132,134,136}Te obtained from the binding energies of neighboring nuclei. To construct the wave functions, (3), of the low-lying 2^+ states up to 2.7 MeV we use only the 2^+ phonons and all one- and two-phonon configurations with energies below 8 MeV for computational convenience. This restriction is justified because this article deals with nuclear states dominated by one-phonon components. In addition, we have checked that the inclusion of high-energy configurations plays a minor role in our calculations.

The calculated transition probabilities represent important fingerprints for the pn symmetry and phonon composition of the 2^+ states. The calculated 2^+ state energies, the largest contributions to the wave function normalization, (5), and the $B(E2)$ and $B(M1)$ values are compared to the experimental data [17,18,35,36] in Table I. Note that the $B(M1)$ values were calculated with free g factors of protons and neutrons. We find a satisfactory description of the isotopic dependence of the $B(E2; 0^+_{gs} \to 2^+_1)$ values near the closed neutron shell $N = 82$. Our calculations describe well the dramatic reduction in the experimental $E2$ excitation strength to the 2^+_1 state upon going from ^{132}Te to ^{136}Te. This reduction is closely related to a predicted simultaneous increase in the $E2$ excitation strength to the 2^+_2 state due to their evolving microscopic structure, which we analyze in the following.

TABLE I. Energies, transition probabilities, and dominant components of phonon structures of the low-lying quadrupole states in ^{132,134,136}Te. Experimental data are taken from Refs. [17,18,35,36].

	$\lambda_i^\pi = 2_i^+$	Energy (MeV)		Structure	$B(E2;\, 0^+_{gs} \to 2^+_i)$ (e^2 fm^4)		$B(E2;\, 2^+_i \to 2^+_1)$ (e^2 fm^4)		$B(M1;\, 2^+_i \to 2^+_1)$ (μ_N^2)	
		Expt.	Theory		Expt.	Theory	Expt.	Theory	Expt.	Theory
^{132}Te	2^+_1	0.974	0.83	$87\%[2^+_1]_{QRPA}$	2160 ± 220	2460				
	2^+_2	1.665	2.33	$79\%[2^+_2]_{QRPA}$						
				$+\ 13\%[2^+_3]_{QRPA}$	100 ± 20	30	0–799	20	>0.23	0.30
	2^+_3	1.788	2.46	$85\%[2^+_4]_{QRPA}$		50		40		0.18
^{134}Te	2^+_1	1.279	2.09	$99\%[2^+_1]_{QRPA}$	1140 ± 130	1380				
	2^+_2	2.464	2.55	$97\%[2^+_2]_{QRPA}$		10		0		0.27
	2^+_3	2.934	2.62	$98\%[2^+_3]_{QRPA}$		0		0		0.10
^{136}Te	2^+_1	0.606	0.92	$97\%[2^+_1]_{QRPA}$	1220 ± 180	1120				
	2^+_2	1.568	2.01	$94\%[2^+_2]_{QRPA}$		740		20		0.51
	2^+_3		2.37	$65\%[2^+_3]_{QRPA}$						
				$+\ 25\%[2^+_4]_{QRPA}$		30		10		0.04

TABLE II. Energies, transition probabilities, and structures of the QRPA quadrupole states in ^{132,134,136}Te.

	State	Energy (MeV)	$B(M1;\, 2_i^+ \to 2_1^+)$ (μ_N^2)	$B(E2;\, 0_{gs}^+ \to 2_i^+)$ (e^2 fm^4)	$\{n_1 l_1 j_1, n_2 l_2 j_2\}_\tau$	X	Y	%
^{132}Te	$[2_1^+]_{\mathrm{QRPA}}$	1.42		2640	$\{1h_{11/2},1h_{11/2}\}_\nu$	1.02	0.26	49
					$\{2d_{5/2},2d_{5/2}\}_\pi$	0.56	0.14	14
					$\{1g_{7/2},1g_{7/2}\}_\pi$	0.65	0.17	20
	$[2_2^+]_{\mathrm{QRPA}}$	2.57	0.48	10	$\{1h_{11/2},1h_{11/2}\}_\nu$	−0.45	0.02	10
					$\{2d_{5/2},2d_{5/2}\}_\pi$	1.29	−0.01	83
					$\{1g_{7/2},1g_{7/2}\}_\pi$	−0.31	0.01	5
	$[2_3^+]_{\mathrm{QRPA}}$	2.63	0.01	0	$\{1g_{7/2},2d_{5/2}\}_\pi$	−0.92	0.00	84
					$\{1g_{7/2},1g_{7/2}\}_\pi$	0.56	−0.01	16
	$[2_4^+]_{\mathrm{QRPA}}$	2.67	0.23	40	$\{1h_{11/2},1h_{11/2}\}_\nu$	−0.82	0.04	34
					$\{1g_{7/2},1g_{7/2}\}_\pi$	1.07	−0.03	57
^{134}Te	$[2_1^+]_{\mathrm{QRPA}}$	2.15		1380	$\{1g_{7/2},1g_{7/2}\}_\pi$	1.05	0.06	55
					$\{2d_{5/2},2d_{5/2}\}_\pi$	0.74	0.06	27
	$[2_2^+]_{\mathrm{QRPA}}$	2.63	0.23	10	$\{1g_{7/2},1g_{7/2}\}_\pi$	−0.89	0.01	40
					$\{1g_{7/2},2d_{5/2}\}_\pi$	0.49	0.00	24
					$\{2d_{5/2},2d_{5/2}\}_\pi$	0.85	0.01	36
^{136}Te	$[2_1^+]_{\mathrm{QRPA}}$	1.05		1010	$\{2f_{7/2},2f_{7/2}\}_\nu$	1.32	0.14	86
					$\{2d_{5/2},2d_{5/2}\}_\pi$	0.32	0.13	4
					$\{1g_{7/2},1g_{7/2}\}_\pi$	0.30	0.12	4
	$[2_2^+]_{\mathrm{QRPA}}$	2.20	0.44	920	$\{2f_{7/2},2f_{7/2}\}_\nu$	−0.52	0.13	13
					$\{2d_{5/2},2d_{5/2}\}_\pi$	0.82	0.04	34
					$\{1g_{7/2},1g_{7/2}\}_\pi$	0.83	0.04	34

The crucial contribution to the wave function of the 2_1^+ states comes from the $[2_1^+]_{\mathrm{QRPA}}$ configuration. The structure of some QRPA phonons is listed in Table II.

The dominant neutron and proton phonon amplitudes X and Y of the 2_1^+ states of ^{132,136}Te are in phase. This is an analogy to the FS states of the IBM-2, although for ^{136}Te we observe the dominance of the neutron configuration $\{2f_{7/2},2f_{7/2}\}_\nu$, which can be interpreted as CIP. As can be seen in Table I, also the wave functions of both the 2_1^+ and the 2_2^+ states of ^{132,134,136}Te are dominated by one-phonon configurations (>87%), which lead to the comparatively small $B(E2;\, 2_2^+ \to 2_1^+)$ values. For the case of ^{132,136}Te the main neutron and proton amplitudes of the $[2_2^+]_{\mathrm{QRPA}}$ states are out of phase. As a consequence, the $B(M1;\, 2_2^+ \to 2_1^+)$ values are remarkable large. They and the opposite phase of the pn contribution support the MS assignments. However, we observe that the value of ^{136}Te is larger than the value of ^{132}Te.

To obtain a better understanding of the mechanism dominating the formation of the $M1$ transition strength between the MS and the 2_1^+ states calculated within the space of one- and two-phonon configurations, we first employ the extreme valence-shell restriction, i.e., the TSM taking into account only the lowest neutron and proton 2QP states. The TSM calculations are performed using the same Skyrme force f_-. Figures 1 and 2 show the results for ^{132}Te and ^{136}Te, respectively. The TSM allows us to discuss only the $M1$ transition, since the 2QP configurations of the giant quadrupole resonance are needed to describe the $B(E2)$ value [37]. As can be seen in Table III, as expected, CIP in the MS and FS states of ^{136}Te is validated by the amplitudes α and β, and no CIP is present in the case of ^{132}Te. This results in a $B(M1)$ value of 1.81 μ_N^2 in ^{132}Te, almost fourteen times larger than that in ^{136}Te.

It is the extension of the variational space to the QRPA phonon configurations that has a strong effect on the $B(M1)$ values. In both nuclei, the origin of this effect is the proximity of the proton $2d_{5/2}$ and $1g_{7/2}$ subshells (Table IV). The closeness of the lowest proton 2QP energies $\{2d_{5/2},2d_{5/2}\}_\pi$, $\{1g_{7/2},2d_{5/2}\}_\pi$, and $\{1g_{7/2},1g_{7/2}\}_\pi$ is reflected in the properties of the QRPA spectrum (see Table II). In both nuclei, the main contribution to the $M1$ matrix element comes from the proton configuration $\{2d_{5/2},2d_{5/2}\}_\pi$. In the case of the 2_1^+ state of ^{132}Te, this configuration exhausts about 44% and 14% of the wave-function normalization within the TSM and the QRPA,

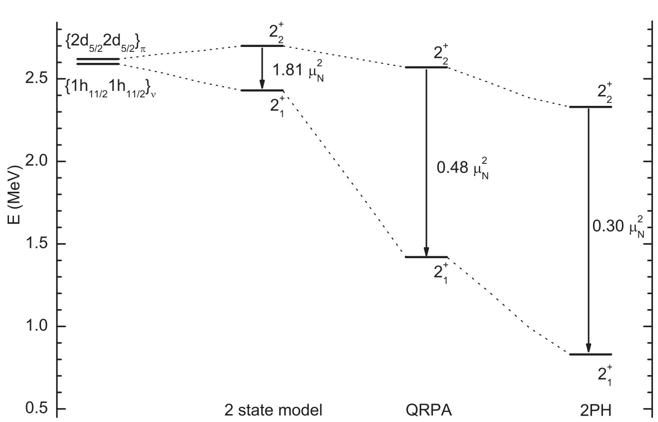

FIG. 1. Energies and $B(M1)$ values of the $2_{1,2}^+$ states in ^{132}Te. The columns “2 state model,” “QRPA,” and “2PH” give values calculated within the two-state model, within the QRPA, and taking into account the phonon-phonon coupling, respectively.

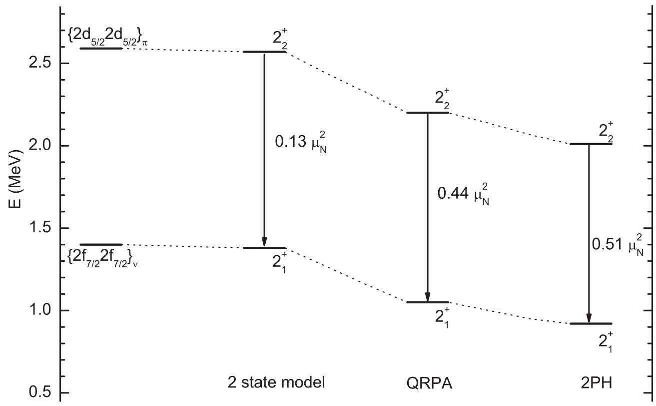

FIG. 2. Energies and B(M1) values of the $2^+_{1,2}$ states in ^{136}Te. The columns "2 state model," "QRPA," and "2PH" give values calculated within the two-state model, within the QRPA, and taking into account the phonon-phonon coupling, respectively.

respectively, causing the strong decrease in the $B(M1)$ value in the QRPA.

In ^{136}Te the $\{2d_{5/2},2d_{5/2}\}_\pi$ contribution to the 2^+_1 state is 4% within the QRPA and only 1.4% in the TSM, hence resulting in the increase in the $B(M1)$ value in the QRPA. The increase in the $B(M1)$ value of ^{136}Te is also related to the considerable increment of the $\{2f_{7/2},2f_{7/2}\}_\nu$ contribution to the wave function of the 2^+_2 state in the QRPA.

We find that the inclusion of two-phonon configurations (see Table I) further changes the aforementioned amplitudes and leads to the $B(M1)$ values of ^{132}Te and ^{136}Te shown in Figs. 1 and 2, respectively. In ^{132}Te, the fragmentation of the $[2^+_1]_{\text{QRPA}}$ configuration reduces the $\{2d_{5/2},2d_{5/2}\}_\pi$ contribution in the structure of the 2^+_1 state, and as a result the $B(M1)$ value is decreased. In ^{136}Te, we find a smaller fragmentation effect, and the wave-function normalizations of the $2^+_{1,2}$ states particularly mix 0.4% of the $[2^+_2]_{\text{QRPA}}$ configuration into the 2^+_1 state and 0.7% of the $[2^+_1]_{\text{QRPA}}$ configuration into the 2^+_2 state. In other words, the $\{2d_{5/2},2d_{5/2}\}_\pi$ contribution in the 2^+_1 state and the $\{2f_{7/2},2f_{7/2}\}_\nu$ contribution in the 2^+_2 state are slightly larger than those in the QRPA. This small change in structure has a large effect on the $B(M1)$ value because of the strong CIP, i.e., small proton contributions in the 2^+_1 state.

As in Refs. [19–25], the neutron dominance of the 2^+_1 state of ^{136}Te leads to the $B(E2)$ anomaly (see Tables I and II). It was shown for the first time in Ref. [19] that the neutron pairing gap in ^{136}Te is smaller than that in ^{132}Te and is key to the pn balance in the 2^+_1 state within the QRPA. The $B(E2)$ anomaly and the isovector character of the 2^+_2 state of ^{132}Te are indispensable

TABLE III. Wave-function amplitudes of the two-state model.

	$\|2^+_\nu\rangle$	$\|2^+_\pi\rangle$	α	β
^{132}Te	$\{1h_{11/2},1h_{11/2}\}_\nu$	$\{2d_{5/2},2d_{5/2}\}_\pi$	0.75	0.66
^{136}Te	$\{2f_{7/2},2f_{7/2}\}_\nu$	$\{2d_{5/2},2d_{5/2}\}_\pi$	0.99	0.12

TABLE IV. Proton single-particle energies (in MeV) near the Fermi energies for ^{132,134,136}Te calculated with Skyrme interactions SLy5 and f_-.

	^{132}Te		^{134}Te		^{136}Te	
	f_-	SLy5	f_-	SLy5	f_-	SLy5
$2p_{1/2}$	−16.4	−16.3	−17.0	−16.9	−17.7	−17.5
$1g_{9/2}$	−14.5	−14.2	−15.2	−14.9	−15.8	−15.5
$1g_{7/2}$	−8.1	−7.9	−8.9	−8.6	−9.4	−9.2
$2d_{5/2}$	−8.1	−7.8	−8.7	−8.4	−9.4	−9.1
$2d_{3/2}$	−5.7	−5.5	−6.4	−6.2	−7.0	−6.8

ingredients in the microscopic analysis. Our calculations with the f_- Skyrme interaction in the particle-hole channel and the volume pairing interaction describe the $E2$ anomaly since the first 2QP state is the $\{1h_{11/2},1h_{11/2}\}_\nu$ state while the second state is the $\{2d_{5/2},2d_{5/2}\}_\pi$ one. The proton SP structure around the Fermi level (Table IV) plays the key role in explaining the predicted effects of the variational-space extension. It is noteworthy that the energy adjacency of the proton subshells $2d_{5/2}$ and $1g_{7/2}$ remains valid for the SLy5 parameter set [38], which is a starting point for the fitting protocol of the f_- set [34]. However, the 2QP state order is not reproduced in the case of the SLy5 set. This is mainly due to less isospin splitting of the effective mass, i.e., $(m^*_n - m^*_p)/m = -0.182$ for the SLy5 set and $(m^*_n - m^*_p)/m = -0.284$ for the f_- set [34].

Previously, shell-model calculations have been performed [39] for ^{132}Te, using the GCN5082 interaction derived from the G matrices. For the 2^+_1 state, $E = 0.953$ MeV, $B(E2\uparrow) = 1615\ \text{e}^2\,\text{fm}^4$, and a 92% dominance of the seniority 2 (i.e., one-phonon) components with 53% neutron contributions and 39% proton ones have been found. Our calculated 2^+_1 energy and the structure are in good agreement but our $B(E2)$ value is somewhat larger, likely due to the effective charges in Ref. [39]. The $B(M1;\, 2^+_2 \to 2^+_1)$ values are in good agreement, but there is a disagreement in the ratios of pn contributions to the 2^+_2 state, with seniority 2 neutron and proton contributions of 35% and 46%, respectively, in Ref. [39]. A possible source of this discrepancy is the different proton SP energy sets in the two approaches.

In summary, by starting from the Skyrme mean-field calculations we have studied the properties of the low-energy spectrum of 2^+ excitations of ^{132,134,136}Te. Using the Skyrme interaction f_- in conjunction with the volume pairing interaction, a successful description of the anomalous behavior of the $B(E2)$ values of the 2^+_1 states is obtained. For ^{132}Te, we identify the 2^+_2 state as a fully developed one-phonon MS state. We observe dominance of the neutron configurations in the wave function of the 2^+_1 state of ^{136}Te. The 2^+_2 state of ^{136}Te is a proton-dominated state, corresponding to an MS state with substantial CIP. Nevertheless, the $B(M1;\, 2^+_{\text{MS}} \to 2^+_1)$ value of ^{136}Te is larger than that of ^{132}Te due to the subtle mechanism based on the near-degeneracy of the proton SP states near the Fermi level. These results suggest the f_- parameter set for the description of MS states and CIP in neutron-rich isotopes.

Data for the low-energy spectrum of 2^+ excitations in ^{132,136}Te are very scarce. It would be desirable to experimentally establish the CIP in the 2_2^+ state identified as the one-phonon MS state, to measure its $B(M1;\, 2_2^+ \to 2_1^+)$ value, and, in particular, the comparatively large $B(E2;\, 2_2^+ \to 0_{gs}^+)$ value as a unique signature, which was previously observed in the stabled ^{92,94}Zr [10–13].

We are grateful to R. V. Jolos, J. Margueron, Nguyen Van Giai, Ch. Stoyanov, A. V. Sushkov, and V. V. Voronov for useful discussions. A.P.S. and N.N.A. thank the Institut für Kernphysik, Technische Universität Darmstadt, where a part of this work was done, for the hospitality. This work was partly supported by the Heisenberg-Landau program, by the DFG under Grant No. SFB634.

[1] F. Iachello and A. Arima, *The Interacting Boson Model* (Cambridge University Press, Cambridge, UK, 1987).
[2] A. Arima *et al.*, Phys. Lett. B **66**, 205 (1977).
[3] T. Otsuka *et al.*, Nucl. Phys. A **309**, 1 (1978).
[4] F. Iachello, Phys. Rev. Lett. **53**, 1427 (1984).
[5] N. Pietralla *et al.*, Phys. Rev. Lett. **83**, 1303 (1999).
[6] N. Pietralla *et al.*, Prog. Part. Nucl. Phys. **60**, 225 (2008).
[7] K. Heyde and J. Sau, Phys. Rev. C **33**, 1050 (1986).
[8] V. Werner *et al.*, Phys. Rev. C **78**, 031301(R) (2008).
[9] J. D. Holt, N. Pietralla, J. W. Holt, T. T. S. Kuo, and G. Rainovski, Phys. Rev. C **76**, 034325 (2007).
[10] V. Werner *et al.*, Phys. Lett. B **550**, 140 (2002).
[11] C. Fransen *et al.*, Phys. Rev. C **71**, 054304 (2005).
[12] E. Elhami *et al.*, Phys. Rev. C **75**, 011301(R) (2007).
[13] E. E. Peters *et al.*, Phys. Rev. C **88**, 024317 (2013).
[14] G. Rainovski *et al.*, Phys. Rev. Lett. **96**, 122501 (2006).
[15] N. Pietralla *et al.*, Phys. Rev. C **58**, 796 (1998).
[16] T. Ahn *et al.*, Phys. Lett. B **679**, 19 (2009).
[17] M. Danchev *et al.*, Phys. Rev. C **84**, 061306(R) (2011).
[18] D. C. Radford *et al.*, Phys. Rev. Lett. **88**, 222501 (2002).
[19] J. Terasaki, J. Engel, W. Nazarewicz, and M. Stoitsov, Phys. Rev. C **66**, 054313 (2002).
[20] A. P. Severyukhin, V. V. Voronov, and N. V. Giai, Phys. Rev. C **77**, 024322 (2008).
[21] N. Shimizu, T. Otsuka, T. Mizusaki, and M. Honma, Phys. Rev. C **70**, 054313 (2004); **74**, 059903(E) (2006).
[22] N. Shimizu *et al.*, J. Phys.: Conf. Ser. **49**, 178 (2006).
[23] D. Bianco, F. Andreozzi, N. Lo Iudice, A. Porrino, and F. Knapp, Phys. Rev. C **85**, 034332 (2012).
[24] D. Bianco, N. Lo Iudice, F. Andreozzi, A. Porrino, and F. Knapp, Phys. Rev. C **86**, 044325 (2012).
[25] D. Bianco, N. Lo Iudice, F. Andreozzi, A. Porrino, and F. Knapp, Phys. Rev. C **88**, 024303 (2013).
[26] T. Mizusaki and T. Otsuka, Prog. Theor. Phys. Suppl. **125**, 97 (1996).
[27] N. Van Giai, C. Stoyanov, and V. V. Voronov, Phys. Rev. C **57**, 1204 (1998).
[28] V. G. Soloviev, *Theory of Atomic Nuclei: Quasiparticles and Phonons* (Institute of Physics, Philadelphia, 1992).
[29] N. Lo Iudice *et al.*, J. Phys. G: Nucl. Part. Phys. **39**, 043101 (2012).
[30] A. P. Severyukhin *et al.*, Eur. Phys. J. A **22**, 397 (2004).
[31] A. P. Severyukhin, N. N. Arsenyev, and N. Pietralla, Phys. Rev. C **86**, 024311 (2012).
[32] P. Ring and P. Schuck, *The Nuclear Many Body Problem* (Springer, Berlin, 1980).
[33] V. V. Voronov, D. Karadjov, F. Catara, and A. P. Severyukhin, Phys. Part. Nucl. **31**, 452 (2000).
[34] T. Lesinski, K. Bennaceur, T. Duguet, and J. Meyer, Phys. Rev. C **74**, 044315 (2006).
[35] R. O. Hughes *et al.*, Phys. Rev. C **71**, 044311 (2005).
[36] B. Fogelberg, B. Ekstrom, L. Sihver, and G. Rudstam, Phys. Rev. C **41**, R1890(R) (1990).
[37] C. Walz *et al.*, Phys. Rev. Lett. **106**, 062501 (2011).
[38] E. Chabanat *et al.*, Nucl. Phys. A **635**, 231 (1998).
[39] K. Sieja, G. Martinez-Pinedo, L. Coquard, and N. Pietralla, Phys. Rev. C **80**, 054311 (2009).